Available online at www.sciencedirect.com
SCIENCE DIRECT®
Biochimica et Biophysica Acta 1617 (2003) 52–61
BIOCHIMICA ET BIOPHYSICA ACTA
BBA
www.bba-direct.com

Intracellular dynamics of the gene delivery vehicle polyethylenimine during transfection: investigation by two-photon fluorescence correlation spectroscopy

Jean-Pierre Clamme, Guruswamy Krishnamoorthy, Yves Mély*

Laboratoire de Pharmacologie et Physico-Chimie des Interactions Cellulaires et Moléculaires, UMR 7034 CNRS, Faculté de Pharmacie, Université Louis Pasteur, Strasbourg 1, 74 Route du Rhin, B.P. 24, F-67401 Illkirch Cedex, France

Received 30 June 2003; accepted 11 September 2003

Abstract

Though polyethylenimine (PEI) is one of the most efficient nonviral vectors, one concern is the significant cytotoxicity of free PEI that represents about 80% of the PEI molecules in PEI/DNA mixtures used for transfection. In this respect, the aim of this work was to further investigate the intracellular fate of PEI during transfection of L929 fibroblasts. To this end, we analyzed by fluorescence correlation spectroscopy (FCS) using two-photon excitation the intracellular concentration and diffusion properties of labeled PEI and PEI/DNA complexes in various compartments of L929 cells. High initial fluorescence intensity, rapid photobleaching and the absence of measurable autocorrelation curves in most selected locations in cytoplasm suggest that PEI/DNA complexes and PEI accumulate (up to 30 times the concentration in the extracellular medium) in late endosomes bound to the inner membrane face. This feature, together with membrane destabilizing properties of PEI, may explain the release of PEI into cytoplasm and subsequent diffusion into the nucleus. In the nucleus, the concentration of PEI was found to be about 2.5- to 3.5-fold higher than the one in the incubation medium. Moreover, autocorrelation curves obtained in the nuclear compartment can be analyzed with either a two-component model (with the major fraction undergoing free Brownian diffusion) or an anomalous diffusion model. Both the endosomal disruption and the large intranuclear PEI concentration may contribute to PEI cytotoxicity.

Keywords: PEI/DNA complex; Anomalous diffusion; Endosome; Photobleaching; Gene therapy

1. Introduction

The success of gene therapy is mainly limited by the development of gene carriers able to promote the delivery of DNA used as a therapeutic agent, to targeted cells. Polyethylenimines (PEI) are among the most promising nonviral gene delivery agents [1,2]. Due to their high cationic charge density, PEIs are proficient condensing agents that lead to the formation of small particles (< 100 nm) [3] exhibiting good transfection efficiency in vitro and in various in vivo applications [4–6]. Nevertheless, despite insights in the preparation of the PEI/DNA complexes [7], selection of PEI with improved physicochemical properties [8,9] and coupling of PEI with ligands [10–13], the efficiency of PEIs is still lower than that of viral vectors and their use for gene therapy still requires further development. Several studies have been performed to determine the mechanism by which PEI/DNA complexes transfect cells and identify the critical steps [14–17]. Even if the transfection mechanism has been shown to depend on the cell type [15], it is established that PEI/DNA complexes are mainly internalized by endocytosis. This internalization is followed by an accumulation of the complexes around the nucleus in late endosomes and lysosomes from which the complexes hardly escape. Moreover, entry of the complexes into the nucleus constitutes an additional bottleneck and its remains unclear if and where dissociation of the complexes occurs during transfection [18]. An additional concern of PEI is its significant cytotoxicity [18–20], which manifests itself by either an immediate (within 2 h) or delayed (between 7 and 9 h posttransfection) cell death. The immediate cell death has been linked to the

* Corresponding author. Tel.: +33-3-90-24-42-63; fax: +33-3-90-24-43-12.
E-mail address: mely@pharma.u-strasbg.fr (Y. Mély).

0005-2736/$ - see front matter © 2003 Elsevier B.V. All rights reserved.
doi:10.1016/j.bbamem.2003.09.002

membrane destabilizing activity of free PEI, which contributes to as much as 85% of the total PEI in the PEI/DNA mixtures used for transfection [21]. Moreover, the delayed cell death has been tentatively attributed to perturbation of nuclear functions by PEI molecules that separate from plasmid DNA in the nucleus.

Due to the detrimental effect of free PEI, it was of interest to further investigate its intracellular fate during transfection of L929 fibroblasts. To this end, we analyzed by two-photon fluorescence correlation spectroscopy (FCS) the intracellular concentration and diffusion properties of rhodamine-labeled PEI during transfection and compared these parameters with those obtained by incubating cells with various amounts of labeled PEI in the absence of DNA. FCS is based on the measurements of fluorescence fluctuations from a microscopic measurement volume (of less than 1 fl) provided either by confocal detection setup or two-photon excitation source (for a review, see Refs. [22,23]). Fluorescent fluctuations are mainly due to diffusion of the fluorescent molecules in and out this volume. Additional fluctuations can arise from any photophysical or chemical process that lead to "blinking" between a fluorescent and a nonfluorescent state during diffusion through the excitation volume. Through a time correlation analysis of the fluorescence fluctuations, the hydrodynamic and photophysical properties are then accessible. In addition, the average number of molecules in the sample volume could also be accessed, making FCS a unique technique to determine intracellular concentrations. Taken together, our data suggest that PEI molecules accumulate in late endosomes and lysosomes where they remain bound to the membrane. Due to the high intraendosomal PEI concentration and the membrane destabilizing properties of PEI, a fraction of the PEI molecules is released in the cytoplasm and diffuse into the nucleus. This leads to an intranuclear concentration that is about 2.5- to 3.5-fold larger than in the incubation medium. Analysis of the autocorrelation curves in the nucleus suggest either that free PEI molecules diffuse in the obstructed intranuclear environment or that part of the PEI molecules may bind to macromolecules and diffuse slowly.

2. Materials and methods

2.1. Chemicals

5-Carboxytetramethylrhodamine (TMR) was purchased from Molecular Probes. Nonlabeled PEI was from Aldrich. TRITC (tetramethylrhodamine isothiocyanate)-labeled PEI (25 kDa) was a gift from J.P. Behr (Illkirch, France). The nonlabeled pCMV-Luc plasmid (5.8 kbp) was amplified by standard molecular biology techniques, using a Jetstar plasmid purification kit (Genomed, Germany) as previously described [15]. The rhodamine-labeled pGeneGrip plasmid (5.1 kbp) was purchased from Gene Therapy Systems (San Diego, USA). Concentrations of DNA stock solutions were determined at 260 nm on a Cary 400 spectrophotometer and plasmid integrity was checked by gel electrophoresis.

2.2. Cell culture

Mouse fibroblasts from the L929 strain (American Tissue Collection, Rockville, MD, USA) were cultured as monolayers in 75 cm^2 culture flasks (Corning Costar, NY, USA) in Dulbecco's modified Eagle's medium (4.5 g/l glucose) (Seromed, Berlin, Germany) supplemented with 10% fetal calf serum (Biowhittaker, Verviers, Belgium), 1 mM sodium pyruvate, 2 mM L-glutamine and antibiotics (penicillin 50 IU/ml, streptomycin 50 mg/ml) (Seromed) in a 8% CO_2 atmosphere, at 37 °C.

2.3. Preparation of complexes and cell transfection

PEI/DNA complexes were prepared in a 25 mM HEPES pH 7.4 buffer as previously described [1]. Briefly, equal volumes of 900 μM PEI (expressed in amine groups) and 90 μM DNA (expressed in phosphate groups) were mixed in order to reach a 45 μM final concentration of DNA and a nitrogen per phosphate (N/P) ratio of 10. Solutions were then briefly vortexed and left for equilibration for a minimum time of 10 min before cell transfection. Prior to transfection, cells were seeded 24 h in two wells Lab-Tek chambered coverglass (Nalge Nunc International, USA) at 7.5×10^4 cells per well in order to reach 1.5×10^5 cells per well after 24 h (~ one division). This concentration allows a high density of cells within the observation field with enough space between cells for individual measurements. After 24 h, the cells were rinsed and supplemented with 1.5 ml of serum-free medium and 200 μl of complexes in order to deliver 4 μg of plasmid for 1.5×10^5 cells. After 2 h incubation, the cells were rinsed and covered with Hank's balanced salt solution (HBSS) for FCS measurement.

2.4. Fluorescence correlation spectroscopy

FCS measurements were performed on a home-build setup as previously described [21]. Briefly, TPE is provided by a Tsunami Ti:Sapphire laser pumped with a Millenia V solid state laser (Spectra-Physics, Mountain View, USA). Pulses of about 100 fs are produced at a wavelength of 850 nm. After a beam expander, the infrared light is focused into the sample by a water immersion Olympus objective (60 ×, NA = 1.2) mounted on an Olympus IX70 inverted microscope. The laser is positioned on the point of interest by moving the sample in the *X* and *Y* directions by a motorized stage (Märzhäuser, Wetzlar, Germany) and in the *Z* direction by moving the objective with a P-721 Pifoc nanopositioner (Polytec PI, Pantin, France). The fluorescence signal from the samples is collected through the objective and directed

by a COWL750 dichroic mirror (Coherent, Santa Clara, USA) toward an 50-μm-diameter optical fiber coupled to an avalanche photodiode (SPCM 200 FC, EG&G, Canada). The residual infrared light is rejected by a BG39 filter (Coherent). The normalized autocorrelation function (ACF), $G(\tau)$, of the fluorescence intensity fluctuations is calculated online by an ALV5000E digital correlator card (ALV, Langen, Germany). Calibration of the system was performed with a 50-nM TMR solution. Assuming a diffusion constant of 2.8×10^{-10} m^2 s^{-1} for TMR [24], the equatorial (r_0) and axial (z_0) radii of the focal volume were found to be of 0.29 and 1.3 μm, respectively, giving an effective measurement volume (V_{eff}) of 0.2 fl.

FCS acquisitions were performed at 4 μm above the cover glass and 5–10 measurements of 15 s were performed for each selected point. Measurement sites in the cytoplasm or in the nucleus were randomly selected and no discrimination of subcompartment in the nucleus was made in this study.

2.5. FCS data analysis

Assuming a three-dimensional Gaussian distributed excitation intensity, the fluorescence ACF of a single freely diffusing species is given by:

$$G_{\text{D}}(\tau) = \frac{1}{N_{\text{app}}}\left(\frac{1}{1+(\tau/\tau_{\text{D}})}\right)\left(\frac{1}{1+(S)^2(\tau/\tau_{\text{D}})}\right)^{1/2} \times \left(1+\frac{Fe^{-\tau/\tau_{\text{t}}}}{1-F}\right) \quad (1)$$

where N_{app} is the mean apparent number of molecules in the excitation volume, S is the ratio between the equatorial and axial radii of the effective two-photon excitation focal volume and τ_{D} is defined as the average residence time of the particles characterized by the diffusion coefficient D ([25]). τ_{t} designates the triplet state lifetime and F is the mean fraction of fluorophores in the triplet state.

In the case of a multicomponent system with species of different quantum yields, a more general form of Eq. (1) may be used [26]:

$$G(\tau) = \sum_{i=1}^{M} q_i^2 N_{\text{app}i}^2 G_{\text{D}i}(\tau) \Bigg/ \left[\sum_{i=1}^{M} q_i N_{\text{app}i}\right]^2 \quad (2)$$

where $N_{\text{app}i}$ and $G_{\text{D}i}(\tau)$ are the mean apparent number and the ACF due to diffusion of the ith species in the focal volume. q_i designates the ratio of the fluorescence yield (given by the product of the detection efficiency by the absorption cross section and the fluorescence quantum yield) of the ith species to that of species 1, taken as a reference.

If the diffusion of the molecules is perturbed by the presence of slow diffusing components, the system can be described by an anomalous diffusion model [27] and Eq. (1) has to be written as [28]:

$$G_{\text{anom}}(\tau) = \frac{1}{N_{\text{app}}}\left(\frac{1}{1+(\tau/\tau_{\text{D}})^{\alpha}}\right)\left(\frac{1}{1+(S)^2(\tau/\tau_{\text{D}})^{\alpha}}\right)^{1/2} \times \left(1+\frac{Fe^{-\tau/\tau_{\text{t}}}}{1-F}\right) \quad (3)$$

where α corresponds to the restriction coefficient. The value of α is equal to 1 for a free Brownian diffusion and decreases when diffusion is obstructed. Moreover, the diffusion coefficient, D_{anom}, which may be calculated from the τ_{D} value describes diffusion without obstacles [29].

FCS data were analyzed with Origin (Microcal, USA) using either a one- or two-population three-dimensional Brownian diffusion model or an anomalous diffusion model.

3. Results

3.1. Fluorescence intensity profiles of intracellular PEI

As a first step to investigate the intracellular diffusion properties of PEI, we incubated L929 cells with rhodamine-labeled PEI concentrations of 53, 26.5 and 13.25 μM (expressed as amine groups) in the absence of plasmid DNA. These PEI concentrations correspond to 1-, 0.5- and 0.25-fold the concentration used to prepare PEI/DNA complexes at a N/P ratio of 10. The cells were incubated with each PEI concentration during 2 h, then rinsed and covered with buffer. In keeping with the reported cytotoxic effects of PEI, many cells appeared rounded, a feature that indicates ill health of cells and corresponds usually to one of the first steps before cell death [18]. The proportion of rounded cells strongly depended on the PEI concentration and reached about 78% for the highest PEI concentration. To investigate the diffusion properties of PEI, the near-IR laser beam was parked at different positions (about 5–10) in selected non-rounded cells (about 5). The excitation volume inside the cell was positioned based on the transmission images and 4 μm above the cover slip. According to the 6-μm height of L929 fibroblasts and the about 1-μm axial radius of the excitation volume, the latter is thought to be fully included in the cell. Moreover, at the 4-μm z-value, any spurious interfering signal from the cover slip is avoided [30]. Both the fluorescence count traces and the autocorrelation curves were recorded for each selected position.

Irrespective of the PEI concentration and the cell selected for measurement, rather high fluorescence intensities could be recorded all over the cell, suggesting that PEI is present all over the cell. Three different cellular compartments could be defined with respect to the fluorescence intensity profile (Fig. 1). The first one is the nucleus where the fluorescence intensity generally oscillates around a mean value with no significant photobleaching (Fig. 1B). This observation could

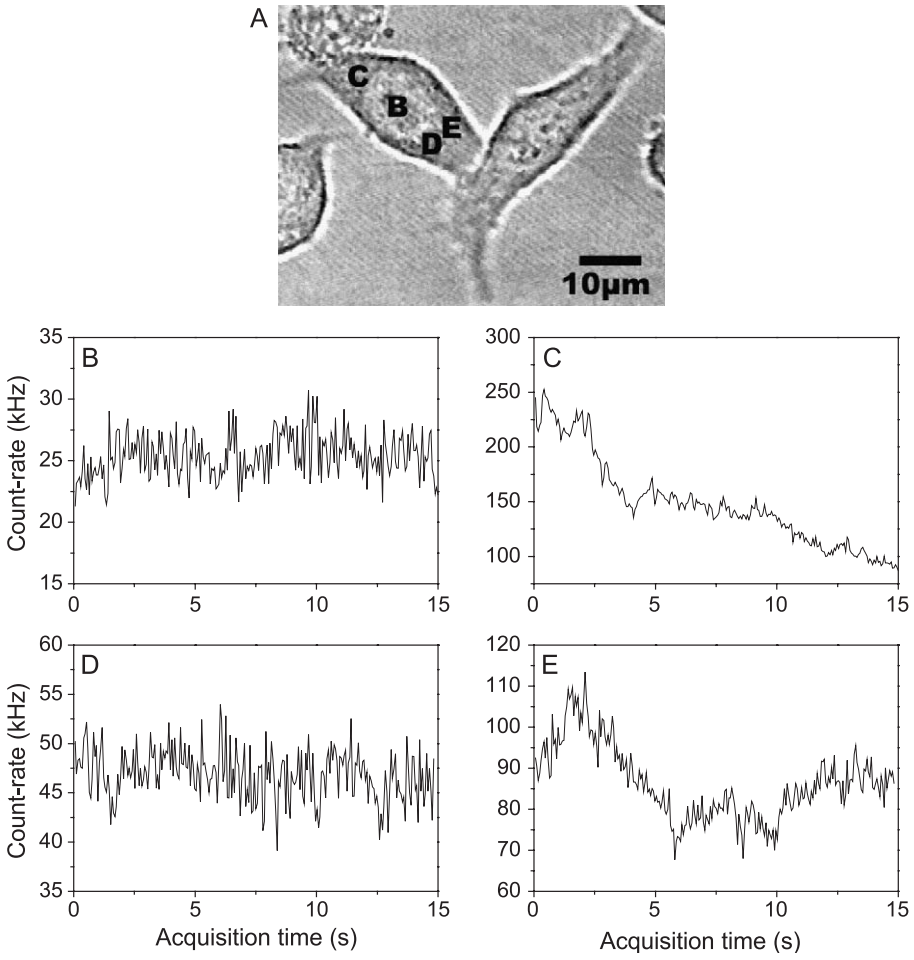

Fig. 1. Intracellular fluorescence count rates in L929 cells challenged with free PEI. The cells were incubated with a 53 μM final concentration of rhodamine-labeled PEI, as described in Materials and methods. (A) Transmission image; (B) representative fluorescence count rates recorded in the nucleus; and (C–E) the cytoplasm.

even be extended to longer illumination periods, since a significant fluorescence decrease is only observed after 5–10 acquisitions at a given point. Additionally, it was observed that the mean fluorescence intensity does not dramatically change all over the nucleus of a given cell, suggesting that PEI may be homogeneously distributed in the nucleus. Moreover, in contrast to the intense spikes observed for instance in the count traces of PEI/DNA complexes in aqueous solution [21], the count traces of nuclear PEI show small and regular variations about the mean fluorescence intensity. This suggests that no complexes or aggregates with a large number of PEI molecules are diffusing in the nucleus. Noticeably, in a few intranuclear locations, a small fluorescence intensity decrease was observed during the two or three first seconds of acquisition (data not shown). By analogy to intranuclear observations performed with labeled oligonucleotides [31], this initial fluorescence decrease may be attributed to PEI molecules that do not move from the excitation volume during the sampling time. The second compartment defined by the count traces is the perinuclear cytoplasmic region. In this compartment, the initial fluorescence intensities of the selected illuminated areas were generally up to 10-fold higher than in the nucleus (Fig. 1C), suggesting that a large number of PEI molecules accumulate in these areas. Moreover, in contrast to the nucleus, the fluorescence intensity drops by about 50–80% during a 15-s acquisition time. When longer acquisition times were used, a continuous fluorescence decrease was observed without reaching a plateau value (data not shown), indicating that PEI molecules accumulate mainly if not exclusively, in nondiffusing or slowly diffusing structures. Since it has been previously reported that PEI accumulates in late endosomes and lysosomes of L929 cells [15], it may be inferred that our observations translate the behavior of PEI molecules in late endosomes and lysosomes. Interestingly, the count traces in a few areas around the nucleus (Fig. 1D) were found to be similar to the intranuclear ones. This suggests that a population of diffusing PEI molecules with behavior similar to that in the nucleus is observable in the perinuclear cytoplasm. Finally, the third compartment defined by the count rate traces is the portion of cytoplasm distant from the

nucleus. The average fluorescence level in this compartment (Fig. 1E) is in between the levels of the nuclear and perinuclear compartments. Moreover, the fluorescence intensity in the third compartment shows large and slow fluctuations. The average duration of these fluctuations is about 5 s and may translate the diffusion of moderately large PEI-containing particles. These particles may tentatively be attributed to early endosomes that have been described in this peripheric cytoplasmic region [15] and which are supposed to be more mobile than the large endosomes around the nucleus.

3.2. Diffusion properties of intracellular PEI

In a next step, the ACF recorded in the three previously defined cellular compartments were analyzed. In the perinuclear compartment, the ACF could generally not be properly analyzed since the continuous decrease in the number of fluorophores due to photobleaching (Fig. 1C) distorts the ACF and leads to staircase-like artifacts [32]. Similarly, the slow and large amplitude oscillations seen in the count traces recorded in the peripheric cytoplasmic regions (Fig. 1E) probably induce corresponding changes in the number of fluorophores that distort ACF and lead to artifacts. It results that only the ACF recorded in the nucleus and in perinuclear areas with nuclear-like count traces could be adequately fitted. In contrast to measurements performed with PEI molecules in aqueous solution [21], the ACF recorded in the nucleus (Fig. 2A) could not be adequately fitted with a one-population model (Eq. (1)) as could be seen from the systematic deviations in the residuals (Fig. 2B). In contrast, an adequate fit (Fig. 2C) was obtained with a two-population model (Eq. (2)), suggesting the existence of both fast and slow diffusing populations. Irrespective of the concentration of PEI incubated with cells, the fast diffusion constant, $D_{fast} = 3.8(\pm 0.1) \times 10^{-11}$ m^2 s^{-1}, was about three times slower than that of PEI in buffer ($D = 1.2(\pm 0.2) \times 10^{-10}$ m^2 s^{-1}) (Table 1). A similar 4- to 5-fold decrease of the diffusion constant in the nucleus with respect to aqueous solution was reported for the green fluorescent protein mutant EGFP [29] and was related to the diffusion of free EGFP molecules in the more viscous intranuclear medium. As a consequence, the fast diffusing population might correspond to free PEI molecules that do not bind to nuclear components and diffuse in a medium similar to that of EGFP. In contrast, the diffusion constant of the slow diffusing population, $D_{slow} = 1.3(\pm 0.1) \times 10^{-12}$ m^2 s^{-1}, was about 100 times slower than that of PEI in aqueous solution, suggesting that this population of PEI may interact with nuclear components and diffuse in a bound form. Alternatively, the autocorrelation data could be adequately fitted with an anomalous diffusion model (Fig. 2D), which assumes obstructed diffusion [28,29]. Irrespective of the PEI concentration incubated with cells, we found a diffusion coefficient, $D_{anom} = 6.7(\pm 0.1) \times 10^{-11}$ m^2 s^{-1} and a restriction coefficient, $\alpha = 0.46 \pm 0.02$. Analysis of the ACF

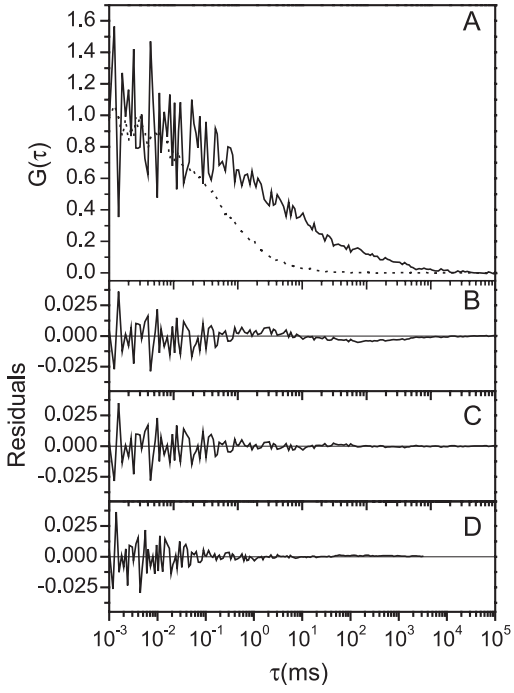

Fig. 2. Autocorrelation curves of PEI in the nucleus of L929 cells. The cells were incubated with free PEI as described in Fig. 1 and the autocorrelation curves were recorded in the nucleus (solid line). The autocorrelation curve of PEI in buffer (dotted line) is given for comparison. Autocorrelations curves were normalized to $N = 1$. Panels B–D represent the residuals obtained by fitting the intranuclear FCS curve with either Eq. (1) (B, one-population, free-diffusion model), Eq. (2) (C, two-population, free-diffusion model) or Eq. (3) (D, anomalous-diffusion model).

recorded in the perinuclear areas with nuclear-like count traces leads to results similar to that of intranuclear ACF (data not shown), suggesting that these areas may correspond to cytoplasmic locations with no endosomes or lysosomes, where PEI molecules diffuse freely.

3.3. Intracellular PEI concentrations

Analysis of the ACF allows the recovering of the average apparent number of molecules present in the focal volume. By dividing this average number by the detection volume, the apparent intracellular concentration of PEI could be deduced at the level of the excitation volume. Since the ACF could only be analyzed in the nucleus and perinuclear areas with nuclear-like behavior, PEI concentrations could thus be only determined in the latter compartments. These FCS-based concentration measurements are straightforward only if all fluorescent molecules show the same fluorescence efficiency and if the signal is free of background [30]. Assuming that all the PEI molecules detected in the excitation volume are characterized by the same fluorescence efficiency and using a background fluorescence, $I_B = 4(\pm 1)$ kHz, the corrected number of molecules, N_{corr}, could be deduced from the apparent number, by $N_{corr} = N_{app}(1 - I_B/I_t)^2$, where I_t is the total fluorescence [33]. Interestingly, N_{corr} was very similar for the anomalous diffusion model

Table1
Intracellular diffusion properties and concentration of PEI measured by FCS on L929 cells incubated with either free PEI or a PEI/DNA mixture

	$[PEI]_{extra}$[a] (μM)	Rounded cells (%)	D_{fast}[a]($\times 10^{11}$) ($m^2\ s^{-1}$)	D_{slow}[a]($\times 10^{11}$) ($m^2\ s^{-1}$)	α[a]	D_{anom}[a]($\times 10^{11}$) ($m^2\ s^{-1}$)	$[PEI]_{nucl}$[a] (μM)
PEI 0.25 ×	13.75	49 (± 9)	4.1 (± 0.6)	1.5 (± 0.4)	0.48 (± 0.01)	7 (± 1)	44 (± 14)
PEI 0.5 ×	26.5	57 (± 6)	3.7 (± 0.7)	1.0 (± 0.3)	0.46 (± 0.01)	6.4 (± 0.6)	98 (± 22)
PEI 1 ×	53	78 (± 5)	3.6 (± 0.5)	1.2 (± 0.3)	0.45 (± 0.01)	7 (± 0.4)	185 (± 26)
Complexes	53	67 (± 11)	3.7 (± 0.1)	1.4 (± 0.3)	0.47 (± 0.02)	6.5 (± 0.7)	143 (± 32)

[a] $[PEI]_{extra}$ and $[PEI]_{nucl}$ are the extracellular and intranuclear concentrations, respectively, of PEI expressed in amine groups. The percentage of rounded cells was determined by counting the number of rounded cells in large-field transmission images. D_{fast} and D_{slow} are the parameters recovered by fitting the ACF in Fig. 2A with Eq. (2). α and D_{anom} are the parameters recovered by fitting the ACF in Fig. 2A with Eq. (3). The intranuclear concentration of PEI was determined as described in the text. Results are expressed as means ± S.E. for about 15–20 measurements performed in three separate experiments.

and the two-population model. Moreover, it appears that the slow diffusing population in the two-population model represents about 20–30% of the PEI molecules. The average apparent number of molecules in both models was about 2.5–3.5 times higher than the number of molecules measured with PEI solutions of the same concentration than that used for incubating the L929 cells. This suggests that L929 cells may actively internalize and concentrate PEI molecules in the nucleus. Moreover, it appears that the nuclear concentration of PEI is similar to that in the perinuclear areas with nuclear-like behavior and proportional to the concentration of PEI in contact with the cells (Table 1). This suggests equilibration of PEI between the perinuclear region and the nucleus.

Additionally, by dividing the average count rate by the number of molecules, we can further deduce the fluorescence per molecule, fpm, and compare it to that obtained with PEI in solution. The nuclear fpm was about 1.2–1.5 kHz and thus, three times less than in solution. This suggests that the nuclear environment may quench to some extent the fluorescence of the rhodamine dye. This conclusion is in contrast with previous reports showing that the intracellular fpm of free rhodamine is similar to that in solution [25]. As a consequence, an alternate hypothesis may be considered in which an additional uncorrelated background fluorescence may decrease the amplitude of the ACF and thus, due to the inverse dependence of the number of molecules on the autocorrelation amplitude,

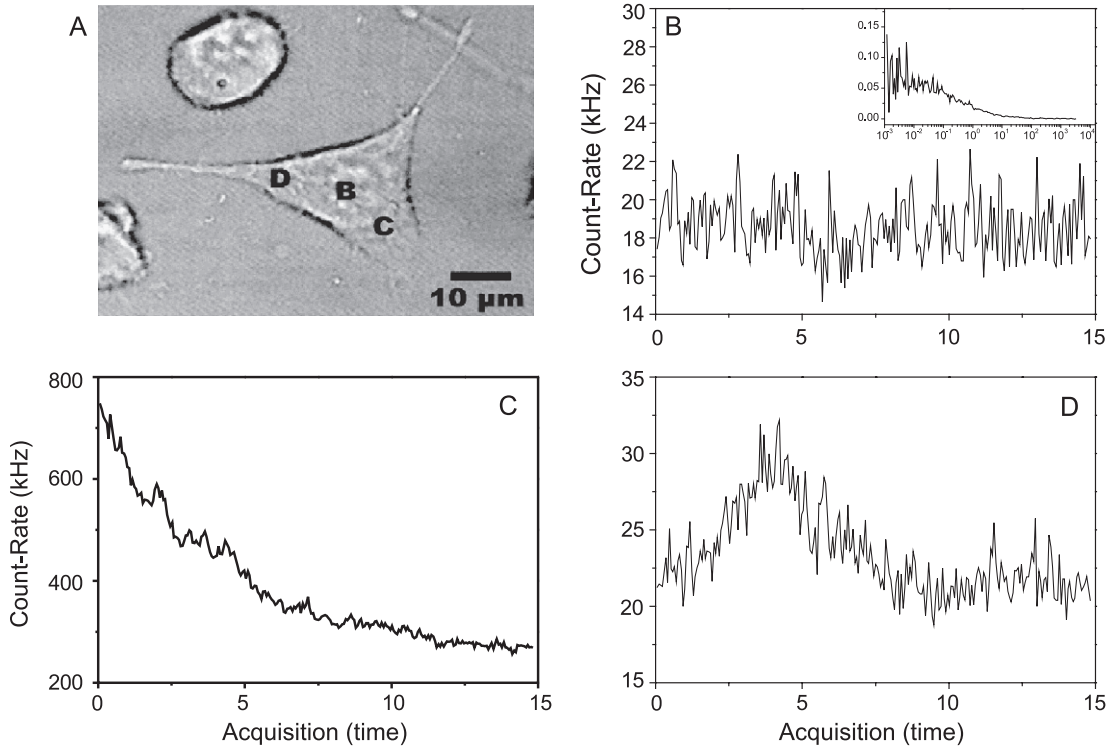

Fig. 3. Intracellular fluorescence count rates in L929 cells incubated with a PEI/DNA mixture. L929 cells (about 1.5×10^5 cells) were incubated with PEI/DNA complexes prepared as described in Materials and methods with final concentrations of plasmid DNA (expressed in phosphate groups) and rhodamine-labeled PEI (expressed in amine groups) of 5.3 and 53 μM, respectively. (A) Transmission image; (B) representative fluorescence count rates recorded in the nucleus; and (C–D) the cytoplasm.

artificially increase the number of molecules and decrease fpm [30]. Assuming that the fpm of rhodamine in cells is identical to that in solution, the total background fluorescence, I_{B1}, might be calculated by:

$$I_{B1} = (2I_t\text{fpm}N_{app} - I_t^2 - [(2I_t\text{fpm}N_{app} - I_t^2)^2 - 4\text{fpm}N_{app}(I_t^2\text{fpm}N_{app} - I_t^3)]^{1/2})/(2\text{fpm}N_{app}) \quad (4)$$

Using this hypothesis, it appears that I_{B1} represents as much as 70–80% of the total fluorescence. This allows then in turn to deduce the corrected number of molecules by $N_{corr}=(I_t - I_{B1})/\text{fpm}$ and thus the corrected concentrations. The latter were found to be rather low and did not exceed 10% of the PEI concentration in the incubation medium (data not shown), suggesting that only a limited PEI concentration would reach the nucleus. The major concern of this hypothesis is the physical origin of this additional background fluorescence. In a previous work, it was associated to immobile molecules binding to the surface of the culture chamber [30]. This hypothesis is unlikely in our case for two reasons. First, the rather high photobleaching power of TPE in the excitation volume [34], which is illustrated in the cytoplasmic count traces (Fig. 1B), would rapidly bleach the immobile molecules. Second, the excitation volume with an axial radius of about 1 μm is set 4 μm above the cover slip and thus cannot excite molecules that would be adsorbed on the cover slip. Accordingly, in the absence of convincing explanation for this background fluorescence, we favor the former hypothesis. The likely compaction of PEI, due to macromolecular crowding, in intracellular compartments could have caused the observed reduction in the value of fpm through interaction between rhodamine groups in PEI.

3.4. Intracellular concentrations and diffusion properties of PEI and PEI/DNA complexes during transfection

In second part of this work, we investigated the intracellular concentrations and diffusion properties of rhodamine-labeled PEI during transfection. L929 cells were challenged with rhodamine-labeled PEI/DNA complexes (prepared at a molar ratio of PEI nitrogen atoms to DNA phosphate of 10) for 2 h and analyzed by FCS after washing. The proportion of rounded cells (Table 1) was intermediate to those observed with the two highest doses of free PEI, in accordance with the presence of large concentrations of free PEI in PEI/DNA mixtures [21]. Moreover, count rate traces and the ACF were also similar to those observed when cells were challenged with free PEI, enabling the definition of the same compartments (Fig. 3A–D). In addition, the intranuclear ACF could again be adequately fitted with either a two-population model or an anomalous diffusion model. The diffusion coefficients and the restriction parameter (Table 1) were indistinguishable from those obtained with free PEI, suggesting that mainly free PEI molecules but not complexes were observed in the nucleus of the selected cells. Moreover, the intranuclear PEI concentration (143 μM) was intermediate to that observed when cells were incubated with either the same or half the concentration of PEI used to prepare the PEI/DNA complexes. In contrast to the nucleus, the high initial count rates observed at given locations of the perinuclear cytoplasm (Fig. 3C) would be well consistent with high local concentrations of PEI and/or PEI/DNA complexes.

Alternatively, we used rhodamine-labeled plasmid to follow the PEI/DNA complexes. Measurements in the perinuclear cytoplasm reveal fast photobleaching areas (Fig. 4A) with no discernable ACF (Fig. 4A, inset). Moreover, after photobleaching, the weak remaining signal was similar to that in nontransfected cells and again did not show any discernable ACF (Fig. 4B, inset). These results confirmed that the labeled DNA molecules contained in complexes in the perinuclear cytoplasm were almost immobile at the FCS time scale. Noticeably, the fluorescence level in the nucleus of the selected cells did not exceed the fluorescence level of control cells, confirming the absence of complexes in the nucleus of these cells. This conclusion is in agreement

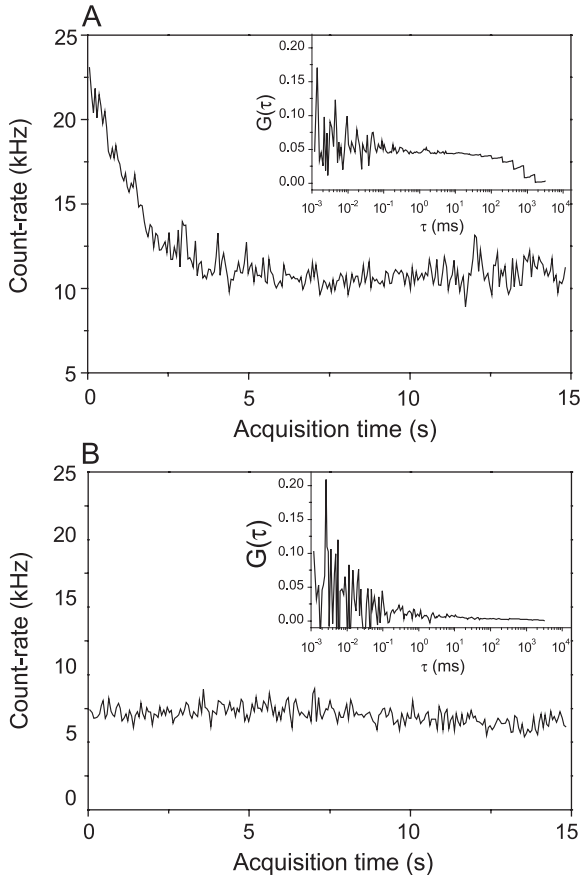

Fig. 4. Intracellular fluorescence count rates and correlation curves (in insert) of L929 cells incubated with mixtures of PEI with rhodamine-labeled plasmid DNA. The concentrations of PEI and plasmid are as in Fig. 3. The count rates and the autocorrelation curves (insert) were recorded in the cytoplasm (A) and the nucleus (B).

with previous confocal studies on the same cells [15], suggesting that DNA molecules may only be transiently present in a small population of cells.

4. Discussion

To get further insight on the cellular mechanism of transfection by mixtures of plasmid DNA with the nonviral vector PEI, we have investigated by two-photon FCS the intracellular diffusion and concentration of the free PEI. These results were compared with those obtained when the cells were challenged with free PEI concentrations that were 1, 0.5 or 0.25 times the PEI concentration used in the PEI/DNA mixture. Both the cytoxicity (as measured from the proportion of rounded cells) and the intranuclear PEI concentration measured with PEI/DNA mixtures were intermediate to those measured with the 1× and 0.5× concentration of free PEI, in line with our previous studies [21] showing that about 85% of PEI molecules are free in PEI/DNA mixtures. Moreover, in agreement with previous confocal [15] or centrifugation [35] data, the FCS-monitored cytoplasmic behavior of the fluorescently labeled PEI either in the absence or in the presence of DNA is fully consistent with internalization by endocytosis, followed by accumulation in late endosomes and lysosomes. Intraendosomal PEI concentration is significantly higher (up to 30 times at certain locations, based on the count rate traces) than the concentration of PEI in the external medium suggesting that PEI molecules are not simply internalized as a part of the extracellular solution. In fact, it is more likely that PEI molecules bind to membrane components as for instance the negatively charged proteoglycans [35]. It follows that due to the small volume of solution internalized in early endosomes, this accumulation of PEI molecules on the external cytoplasmic leaflet leads to a PEI concentration increase as compared to the external medium. The binding of PEI to membrane components was confirmed in late endosomes. Indeed, in contrast to early endosomes, late endosomes are sufficiently large with respect to the excitation volume that intraendosomal diffusion of free particles could be discriminated from the diffusion of particles bound to the inner surface of the membrane [36]. By analogy with the behavior of a minor population of labeled latex microparticles incubated with endothelial cells [36], the strong photobleaching in late endosomes strongly suggest that PEI molecules remain bound to the inner surface of endosome membranes and thus diffuse at the low speed of the endosomes themselves. By analogy to PEI molecules, the strong photobleaching and the absence of detectable diffusion in the late endosomes of cells incubated with labeled PEI/DNA complexes further suggest that the complexes also remain bound to the endosome membranes. Alternatively, the diffusion of PEI/DNA complex could have been hindered to an extent such that it is not observable in the FCS time scale. It should be mentioned that the diffusion time of PEI/DNA complexes in free solution is ~ 2 ms ($D \sim 6 \times 10^{-12}$ $m^2\ s^{-1}$ [21]) and hence its hindered diffusion in cells could have slowed it beyond the observable time scale.

The observation of cytoplasmic areas with freely diffusing PEI molecules and the detection of significant intranuclear PEI concentrations additionally suggest that PEI is released from the endosomes. This may be a consequence of the membrane destabilizing properties of PEI. Indeed, PEI was reported to permeabilize Gram negative bacterial outer membranes [37,38], and to disrupt liposomal membranes made from phosphatidyl serine [39] as well as lysosomes [40]. This last effect was found to strongly depend on PEI concentration. While a PEI concentration representative of the concentrations used to transfect cells showed only small effects, an important lysosomal disruption was obtained at 5-fold higher concentrations. In this respect, the inferred high intraendoensomal PEI concentrations may be sufficient to destabilize the endosomes, while in line with previous results on neuronal cells [41], the extracellular PEI concentration may not be sufficient to destabilize the plasma membrane. The accumulation of PEI on the inner surface of endosome membranes together with the membrane-destabilizing properties of PEI may by themselves explain the release of PEI into the cytoplasm. This would constitute a mechanism alternative to the osmotic swelling hypothesis [1]. In the latter hypothesis, it is thought that due to the buffering capacity of PEI, a massive accumulation of protons followed by a passive chloride influx could generate an osmotic swelling and subsequent endosome disruption. However, since the major part of PEI in PEI/DNA mixtures is free and since the pK value of PEI is ~ 8.4 [42], only a limited buffering capacity is expected at the low pH values in late endosomes or lysosomes, and hence osmotic swelling is unlikely to play a significant role in endosome disruption.

In a next step, the PEI released by the endosomes may diffuse through the nuclear pores. This hypothesis is reasonable since the average molecular weight of PEI (25 kDa) is significantly below the exclusion limit for passive transport through the nuclear pore complex [43]. Moreover, the identification of a few cytoplasmic perinuclear areas where the concentration of PEI is in the same range than the intranuclear one further suggests that the intranuclear PEI concentration equilibrates with the cytoplasmic concentration of released PEI. Noticeably, the scarcity of these cytoplasmic areas with released PEI is in line with the large volume occupied by the late endosomes and lysosomes around the nucleus [15]. The presence of PEI molecules in the nucleus is consistent with previous observations on EA.hy 926 cells [14], except that the PEI molecules do not seem to accumulate in organized areas but were homogeneously distributed in the nucleus. This suggests that as for PEI internalization [15], there may be some cellular dependence on the distribution of PEI in the nucleus. Moreover, the absence of photobleaching in the nucleus together with the reported absence of cellular diffusion for DNA molecules larger than 1000 kDa [44] strongly suggest that PEI

molecules do not bind to the host genome in the nucleus. The absence of binding of PEI to DNA in the nucleus could be due to packing and condensation of nuclear DNA by histones. This further suggests that incorporation of the imported DNA into the chromosomal DNA would require a nontrivial mechanism whereby the imported DNA is extracted from the PEI/DNA complex.

The diffusion of PEI molecules could be adequately described by either a two-population or an anomalous-diffusion model. In the first model, the major fraction of PEI molecules was found to diffuse in a free form. In good agreement with measurements performed on EGFP and TMR molecules [25,29], the apparent intranuclear viscosity was found to be about three times larger than that of the buffer. In contrast, such a high viscosity was not evidenced for small oligonucleotides [31], suggesting either that oligonucleotides do not diffuse in the same nuclear compartments than TMR, EGFP and PEI or that the latter molecules interact more strongly with their environment than oligonucleotides. The second population of PEI molecules diffuses with a much smaller diffusion constant, suggesting that it may diffuse in a bound form. Similar diffusion constants were reported for a population of oligonucleotides diffusing in the nucleus and were associated to the diffusion of oligonucleotides bound to large macromolecular complexes [31]. In the anomalous-diffusion model, the PEI molecules are thought to diffuse in an obstructed medium and thus show an inhomogeneously retarded diffusion [25,29]. The obstacles may be constituted by the chromatin and the associated macromolecules organized in chromosomes. A similar model was applied to the intranuclear diffusion of EGFP, TMR and small peptides [25,29,30]. Interestingly, the restriction coefficient ($\alpha = 0.46$) for PEI was similar to that (0.5) of TMR [25] but much smaller than that (0.8) of EGFP [29] and cell-permeable peptides [30]. Since α is equal to 1 for free diffusion and decreases with increasing obstacle concentration, it may be concluded that PEI and TMR either diffuse in more obstructed areas or interact more strongly with the obstacles than peptides or proteins. This last hypothesis could be readily explained by the high density of positive charges that may favor the interaction of PEI with the negatively charged intranuclear macromolecules. In a third model, we could assign the multicomponent diffusion kinetics of PEI to multiple compartments in the nucleus. In addition, the absence of PEI/DNA complexes in the nucleus of the observed L929 cells may be related to the low transfection efficiency of these complexes since only a few percent of L929 cells have been shown to express the transgene [15].

Another important feature pointed out by our measurements is that the intranuclear PEI concentration is proportional to the concentration of PEI incubated with the L929 cells. This suggests that the initial binding of PEI to the plasma membrane is proportional to the external PEI concentration and that no saturation occurs in the tested concentration range. Since similar intranuclear PEI concentrations were found in normal and rounded cells (data not shown), it may be further concluded that PEI cytotoxicity in the latter cells is not related to a massive release of PEI from the endosomes. It is likely that the concentrations of free PEI measured in the cytoplasm or nucleus are themselves cytotoxic. In keeping with this hypothesis, the percentage of rounded cells was found to linearly correlate with the intranuclear concentration of PEI (Fig. 5) for all the measurement points including the one performed with the PEI/DNA mixture. Moreover, it could be further concluded from Fig. 5 that the intranuclear PEI concentration giving 50% toxicity is about 60 μM. It should be noted that the cytotoxic effects of PEI on L929 cells occur in less than 2 h and in contrast to EA.hy926 cells [18] do not markedly change with time (data not shown). Immediate cytotoxicity seems thus to be prevalent in L929 cells. It may be speculated that this toxicity is related to the permeabilization of late endosomes and lysosomes. Additionally, free PEI molecules in the cytoplasm and the nucleus may interfere with proteins and perturb critical cell functions. Additional work is required to identify the cellular targets of free PEI.

In summary, we have shown in the present work that after endocytosis, the PEI molecules and the PEI/DNA complexes remain bound to the endosome membranes. The binding of PEI to the plasma membrane seems highly efficient since the endosomal PEI concentration was found to be much larger than the external concentration of PEI in contact with the cells. Due to the membrane-destabilizing properties of PEI and the dependence of these properties with PEI concentration, this may lead to a release of PEI in the cytoplasm and a diffusion of free PEI into the nucleus. Inside the nucleus, the PEI molecules do not bind to the host genome but rather remain free and diffuse in an obstructed environment. However, it cannot be excluded that a significant fraction of PEI molecules bind to some still unidentified macromolecules and diffuse in a bound form. The

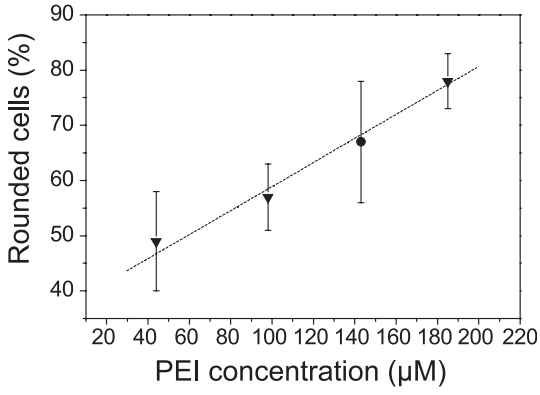

Fig. 5. Correlation between cytotoxicity and intranuclear PEI concentration. Cytotoxicity was evaluated from the percentage of rounded L929 cells counted in the Lab-Tek chambered coverglass when the cells were incubated with either free PEI (▼) or PEI/DNA mixture (●). Intranuclear PEI concentrations were from Table 1.

absence of binding of PEI to the host genome suggests that the latter does probably not trigger the dissociation of PEI/DNA complexes entering into the nucleus. Both the release of PEI in the cytoplasm and the large concentration of PEI in the nucleus may contribute to the cytotoxic effects of PEI.

Acknowledgements

This work was supported by the Association française contre les myopathies and Association pour la Recherche contre le Cancer. J.P.C. and G.K. are fellows from the Ligue Régionale du Bas-Rhin et du Haut-Rhin contre le Cancer and Ministère de la Recherche, respectively.

References

[1] O. Boussif, F. Lezoualc'h, M.A. Zanta, M.D. Mergny, D. Scherman, B. Demeneix, J.P. Behr, Proc. Natl. Acad. Sci. U. S. A. 92 (1995) 7297–7301.
[2] B. Abdallah, A. Hassan, C. Benoist, D. Goula, J.P. Behr, B.A. Demeneix, Hum. Gene Ther. 7 (1996) 1947–1954.
[3] M.X. Tang, F.C. Szoka, Gene Ther. 4 (1997) 823–832.
[4] D. Goula, C. Benoist, S. Mantero, G. Merlo, G. Levi, B.A. Demeneix, Gene Ther. 5 (1998) 1291–1295.
[5] J.L. Coll, P. Chollet, E. Brambilla, D. Desplanques, J.P. Behr, M. Favrot, Hum. Gene Ther. 10 (1999) 1659–1666.
[6] A.C. Hirko, D.D. Buethe, E.M. Meyer, J.A. Hughes, Biosci. Rep. 22 (2002) 297–308.
[7] M. Ogris, P. Steinlein, M. Kursa, K. Mechtler, R. Kircheis, E. Wagner, Gene Ther. 5 (1998) 1425–1433.
[8] M. Ogris, P. Steinlein, S. Carotta, S. Brunner, E. Wagner, AAPS PharmSciTech 3 (2001) E21.
[9] L. Wightman, R. Kircheis, V. Rossler, S. Carotta, R. Ruzicka, M. Kursa, E. Wagner, J. Gene Med. 3 (2001) 362–372.
[10] R. Kircheis, A. Kichler, G. Wallner, M. Kursa, M. Ogris, T. Felzmann, M. Buchberger, E. Wagner, Gene Ther. 4 (1997) 409–418.
[11] P. Erbacher, T. Bettinger, P. Belguise-Valladier, S. Zou, J.L. Coll, J.P. Behr, J.S. Remy, J. Gene Med. 1 (1999) 210–222.
[12] R. Kircheis, L. Wightman, A. Schreiber, B. Robitza, V. Rossler, M. Kursa, E. Wagner, Gene Ther. 8 (2001) 28–40.
[13] M. Thomas, A.M. Klibanov, Proc. Natl. Acad. Sci. U. S. A. 99 (2002) 14640–14645.
[14] W.T. Godbey, K.K. Wu, A.G. Mikos, Proc. Natl. Acad. Sci. U. S. A. 96 (1999) 5177–5181.
[15] A. Remy-Kristensen, J.P. Clamme, C. Vuilleumier, J.G. Kuhry, Y. Mely, Biochim. Biophys. Acta 1514 (2001) 21–32.
[16] A. Kichler, C. Leborgne, E. Coeytaux, O. Danos, J. Gene Med. 3 (2001) 135–144.
[17] M.L. Forrest, D.W. Pack, Mol. Ther. 6 (2002) 57–66.
[18] W.T. Godbey, K.K. Wu, A.G. Mikos, Biomaterials 22 (2001) 471–480.
[19] D. Fischer, T. Bieber, Y. Li, H.P. Elsasser, T. Kissel, Pharm. Res. 16 (1999) 1273–1279.
[20] D. Putnam, R. Langer, Macromolecules 32 (1999) 3658–3662.
[21] J.P. Clamme, J. Azoulay, Y. Mely, Biophys. J. 84 (2003) 1960–1968.
[22] S.T. Hess, S. Huang, A.A. Heikal, W.W. Webb, Biochemistry 41 (2002) 697–705.
[23] O. Krichevsky, G. Bonnet, Rep. Prog. Phys. 65 (2002) 251–297.
[24] D. Magde, E.L. Elson, W.W. Webb, Biopolymers 13 (1974) 29–61.
[25] P. Schwille, U. Haupts, S. Maiti, W.W. Webb, Biophys. J. 77 (1999) 2251–2265.
[26] N. Thompson, in: R. Lakowicz (Ed.), Topics in Fluorescence Spectroscopy, vol. 1. Plenum, New York, 1991, pp. 337–378.
[27] J.-P. Bouchaud, A. Georges, Phys. Rep. 195 (1990) 127–293.
[28] P. Schwille, J. Korlach, W.W. Webb, Cytometry 36 (1999) 176–182.
[29] M. Wachsmuth, W. Waldeck, J. Langowski, J. Mol. Biol. 298 (2000) 677–689.
[30] T. Waizenegger, R. Fischer, R. Brock, Biol. Chem. 383 (2002) 291–299.
[31] J.C. Politz, E.S. Browne, D.E. Wolf, T. Pederson, Proc. Natl. Acad. Sci. U. S. A. 95 (1998) 6043–6048.
[32] R. Brock, M.A. Hink, T.M. Jovin, Biophys. J. 75 (1998) 2547–2557.
[33] D.E. Koppel, Phys. Rev., A, Gen. Phys. 10 (1974) 1938–1945.
[34] G.H. Patterson, D.W. Piston, Biophys. J. 78 (2000) 2159–2162.
[35] M. Lecocq, S. Wattiaux-De Coninck, N. Laurent, R. Wattiaux, M. Jadot, Biochem. Biophys. Res. Commun. 278 (2000) 414–418.
[36] N. Yoshida, M. Kinjo, M. Tamura, Biochem. Biophys. Res. Commun. 280 (2001) 312–318.
[37] I.M. Helander, K. Latva-Kala, K. Lounatmaa, Microbiology 144 (Pt 2) (1998) 385–390.
[38] I.M. Helander, H.L. Alakomi, K. Latva-Kala, P. Koski, Microbiology 143 (Pt 10) (1997) 3193–3199.
[39] N. Oku, N. Yamaguchi, S. Shibamoto, F. Ito, M. Nango, J. Biochem. (Tokyo) 100 (1986) 935–944.
[40] A.R. Klemm, D. Young, J.B. Lloyd, Biochem. Pharmacol. 56 (1998) 41–46.
[41] R.C. Lambert, Y. Maulet, J.L. Dupont, S. Mykita, P. Craig, S. Volsen, A. Feltz, Mol. Cell. Neurosci. 7 (1996) 239–246.
[42] A. von Harpe, H. Petersen, Y. Li, T. Kissel, J. Control. Release 69 (2000) 309–322.
[43] R. Peters, EMBO J. 3 (1984) 1831–1836.
[44] A.S. Verkman, Trends Biochem. Sci. 27 (2002) 27–33.